Facile Formation of Gold Nanoparticles on Periodic Mesoporous Bipyridine-silica

Nobuhiro Ishito[a,b], Kiyotaka Nakajima[a,b], Yoshifumi Maegawa[c,d], Shinji Inagaki[c,d], Atsushi Fukuoka[a,b,*]

[a] Institute for Catalysis, Hokkaido University, Sapporo, Hokkaido 001-0021 (Japan)

[b] Graduate School of Chemical Sciences and Engineering, Hokkaido University, Sapporo, Hokkaido 060-8628 (Japan)

[c] Toyota Central R&D Laboratories, Inc., Nagakute, Aichi 480-1192 (Japan)

[d] Japan Science and Technology Agency (JST)/ACT-C, Nagakute, Aichi 480-1192 (Japan)

KEYWORDS: gold nanoparticles, metal complex, periodic mesoporous organosilica

Abstract

Silica-supported gold nanoparticles (AuNPs) can be synthesized on a bipyridine incorporated periodic mesoporous organosilica (BPy-PMO) as an inorganic support. Reaction of a bipyridine group in the periodic mesoporous organosilica with $HAuCl_4$ forms an $AuCl_2$-based complex, and its structure corresponds to a homogeneous complex, $[AuCl_2(bpy)]Cl$. Thermal reduction of the complex in H_2 results in the formation of small gold nanoparticles with an average size of ca. 3.8 nm. Combined with nitrogen adsorption, XRD, UV/Vis, TEM, and XAFS measurements, it is demonstrated that uniform gold nanoparticles are homogeneously distributed inside mesopores. The size and distribution of gold nanoparticles is mainly controlled by strong interaction of surface metallic Au with pore walls of the periodic mesoporous organosilica. AuNPs/BPy-PMO shows higher catalytic activity than Au/MCM-41 in aerobic oxidation of benzaldehyde.

1. Introduction

Gold nanoparticles (AuNPs) have been widely studied as a promising material for catalysis, electronic and photonic device, and drug delivery system [1-7]. Despite bulk Au metal has no functionality for catalysis, gold particles in nanometer-scale show very

unique activity for a variety of reactions, which is represented by low temperature oxidation of CO with O_2 [8,9]. Because catalytic performance of AuNPs strongly depends on their particle size, Haruta et al. developed the deposition precipitation method to form highly dispersed AuNPs on various metal oxide supports [8,10]. This method is solely based on impregnation of preformed $Au(OH)_3$ with inorganic supports, and it is able to control the size of resultant AuNPs by optimization of pH in solution containing $HAuCl_3$ precursor. In contrast, direct impregnation of ionic gold precursors on inorganic supports and subsequent reduction to form AuNPs is not simply accomplished by a conventional combination of evaporation and reduction technique, owing to low affinity of Au with the supports resulting in the formation of large Au particles. A variety of methods were reported for the preparation of supported AuNPs catalysts such as co-precipitation [11], photochemical synthesis [12], solid-solid reactions of a gold complex with the supports [13], liquid-phase reduction [14,15], and impregnation of AuNPs stabilized with sulfur or phosphorus-containing organic compounds and polymers [16-18]. Fe_2O_3 and TiO_2 are useful supports for the preparation of well-defined AuNPs; however, silicas with high surface area, which are widely used as supports for organic functional groups and novel metals, are not applicable as host materials due to difficulties in controlling the size below 6 nm.

Periodic mesoporous organosilicas (PMOs) are unique mesoporous materials that consist of crystal-like ordered arrays of organic moieties bridged by siloxane bonds [19,20]. Introduction of organic groups into the PMOs can lead to various chemical and physical properties [21-23]. Recently, a PMO with 2,2'-bipyridyl (BPy) groups has been synthesized from a bridged precursor, 5,5'-bis(triisopropoxysilyl)-2,2'-bipyridine, in the presence of a structure-directing agent. 2,2'-Bipyridyl group incorporated into siloxane network is a versatile ligand and readily available as a chelating unit for the formation of Ir, Ru, Re, and Pd complexes [24-26]. Herein, we report a novel strategy for the immobilization of AuNPs on BPy-PMO through the formation of Au complex with surface BPy moiety and subsequent thermal reduction. First, an Au complex was formed by the treatment of BPy-PMO with $HAuCl_4 \cdot 4H_2O$ in ethanol. These complexes are easily transformed to AuNPs by a simple reduction with thermal treatment of the Au complex-stabilized BPy-PMO with H_2. Results of characterization and catalysis of AuNPs/BPy-PMO are also presented.

2. Experimental

2.1. Reagents

$HAuCl_4 \cdot 4H_2O$ was purchased from Wako Pure Chemical Industries, Ltd. Other

reagents were obtained with the highest grade and used without further purification.

2.2. Synthesis of BPy-PMO supported AuNPs

BPy-PMO was synthesized using 5,5'-bis(triisopropoxysilyl)-2,2'-bipyridine as a bridged silica precursor and octadecyltrimethylammonium chloride as a surfactant [24]. An Au complex immobilized BPy-PMO, denoted $AuCl_3$-BPy-PMO, was prepared from BPy-PMO and $HAuCl_4 \cdot 4H_2O$ as follows: a 100 mg of BPy-PMO was added to a mixture of EtOH (30 mL) and $HAuCl_4 \cdot 4H_2O$ (100 mg, 0.50 mmol) under an Ar atmosphere. After stirring the mixture under reflux condition for 6 h, the resulting solid was filtered, washed with excess amounts of EtOH, and dried at 298 K in vacuo to afford $AuCl_3$-BPy-PMO (110 mg) as a pale yellow powder. The solid was conducted with thermal reduction in H_2 at 423 K for 1 h to give BPy-PMO-supported AuNPs which is denoted AuNPs/BPy-PMO. For comparison, an MCM-41-supported AuNPs was prepared by a conventional impregnation method using $HAuCl_4 \cdot 4H_2O$. After immobilization of Au species on MCM-41 by vacuum evaporation at 298 K, the dried sample was also reduced in H_2 at 423 K for 1 h to obtain MCM-41-supported AuNPs (Au/MCM-41). A model complex for $AuCl_3$-BPy-PMO, $[AuCl_2(bpy)]Cl$, was synthesized according to a procedure in the literature [27] and purified by

recrystallization.

The samples were characterized using UV/Vis diffuse reflectance spectroscopy (UV/Vis DRS; Jasco, V-650), X-ray fluorescence spectroscopy (XRF, Shimadzu EDX-720), nitrogen adsorption (MicrotracBEL Belsorp-mini II), X-ray diffraction (XRD, Rigaku Ultima IV, Cu Kα), transmission electron microscopy (TEM, JEOL JEM-2100F, 200 kV), and X-ray absorption fine structure (XAFS, BL14B2 of SPring-8).

2.3. Oxidation of benzaldehyde with supported AuNPs

A mixture of benzaldehyde (11 mg, 0.1 mmol), catalyst (10 mg), $NaHCO_3$ (17 mg, 0.2 mmol), and distilled water (5.0 mL) were placed into a Pyrex vial (20 mL) and stirred at 303 K for 2 h with bubbling of oxygen gas at a flow rate of 10 mL min^{-1}. After the reaction, the mixture was analyzed using gas chromatography (GC; Shimadzu GC-14B, flame ionization detector) with an HR-20m (0.25 mm diameter, 30 m long) column. Naphthalene was used as an internal standard in this experiment.

3. Results and Discussion

3.1. Synthesis of Au complex on BPy-PMO

The formation of gold complexes by thermal treatment of BPy-PMO with $HAuCl_4 \cdot 4H_2O$ in ethanol (Scheme 1) were confirmed by Au L_3-edge XAFS measurement, which provides information on the electronic state and structure of Au species stabilized on the support. In the X-ray absorption near-edge structure (XANES) in Fig. 1a, the edge energy of Au species on $AuCl_3$-BPy-PMO appeared at 11917 eV which corresponds to a trivalent Au species. Because $AuCl_3$-BPy-PMO and $[AuCl_2(bpy)]Cl$ show almost the same spectra, electronic structure of Au atoms in $AuCl_3$-BPy-PMO is the same as that of trivalent Au species in $[AuCl_2(bpy)]Cl$. This trend was also observed for extended X-ray absorption fine structure (EXAFS) oscillation (Fig. 1b) and Fourier transforms of EXAFS (Fig. 1c); $AuCl_3$-BPy-PMO gave almost the same spectrum as $[AuCl_2(bpy)]Cl$. These results show that a similar structure to that of the corresponding homogeneous complex, $[AuCl_2(bpy)]Cl$, is successfully formed on the surface of BPy-PMO via a BPy group as a chelating unit as shown in Fig. 1d.

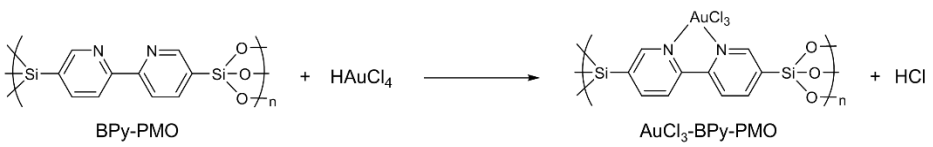

Scheme 1. Formation of Au complex on BPy-PMO.

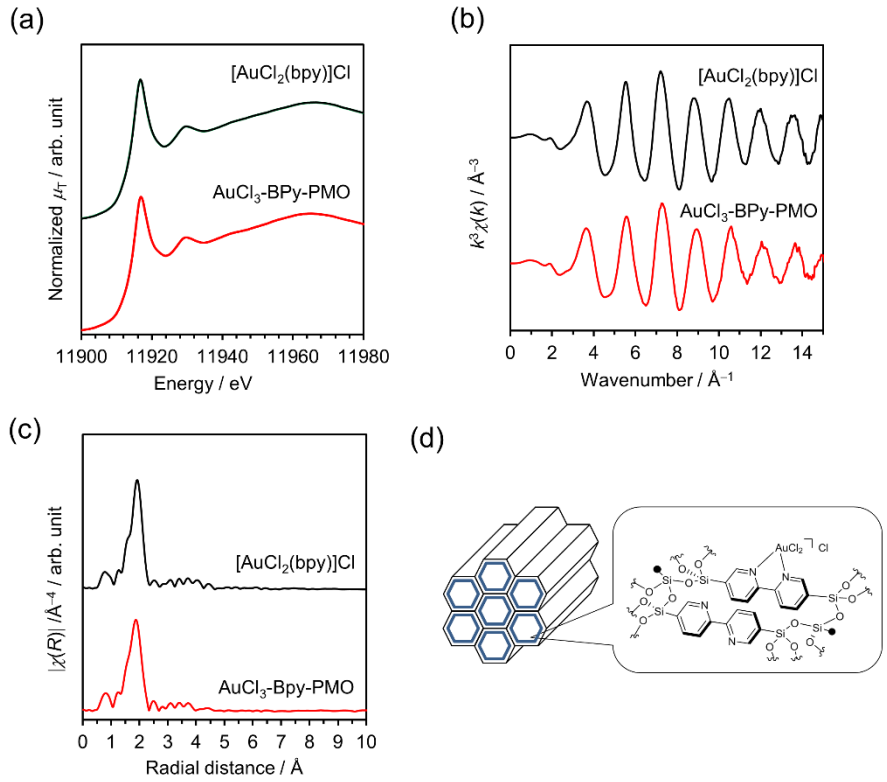

Fig. 1. (a) Au L_3-edge XANES, (b) EXAFS oscillation, (c) Fourier transforms of EXAFS spectra for $AuCl_3$-BPy-PMO (red line) and [$AuCl_2$(bpy)]Cl (black line), and (d) proposed structure of $AuCl_3$-BPy-PMO.

3.2. Formation of Au nanoparticles on BPy-PMO

We performed thermal reduction of $AuCl_3$-BPy-PMO at 423 K in H_2 to obtain BPy-PMO-supported AuNPs. Fig. 2 shows N_2 adsorption-desorption isotherms and non-linear DFT (NLDFT) pore size distribution curves of bare BPy-PMO and AuNPs/BPy-PMO. Both bare BPy-PMO and AuNPs/BPy-PMO have type-IV isotherms

with no pronounced hysteresis loops, and this result is typical of mesoporous materials with small-sized mesopores (Fig. 2a) [28]. NLDFT calculation with the isotherms provides pore size distribution curves of these samples, which reveals the presence of uniform mesopores of ca. 4.4 nm in diameter (Fig. 2b). While Brunauer–Emmett–Teller (BET) surface area slightly decreased from 670 to 620 $m^2 g^{-1}$, it is apparent that original mesoporosity of BPy-PMO retained intact after the formation of Au complex and subsequent H_2 reduction. Fig. 3 shows XRD patterns of bare BPy-PMO and AuNPs/BPy-PMO in (a) low and (b) high-angle regions. There is one intense diffraction at $2\theta = 1.69^\circ$ that can be assigned to (100) plane of *p6mm* symmetry for mesoporous arrangement. Despite the presence of some diffractions due to periodic structure of BPy units in high-angle region, there are no signals of Au metal, suggesting the formation of small nanoparticles undetectable by XRD measurement. The amount of Au loaded on BPy-PMO was estimated to be 1.1 wt% by EDX analysis.

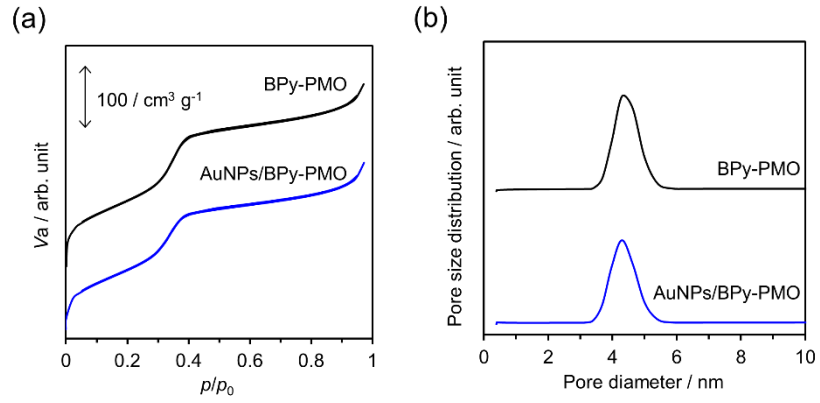

Fig. 2. (a) N_2 adsorption isotherms and (b) NLDFT pore diameter distribution curves of BPy-PMO (black line) and AuNPs/BPy-PMO (blue line).

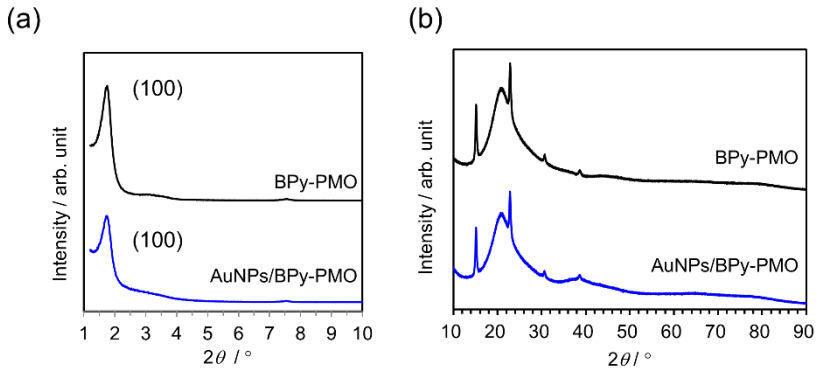

Fig. 3. XRD patterns of BPy-PMO (black line) and AuNPs/BPy-PMO (blue line) in (a) low and (b) high-angle region.

As a control experiment, MCM-41-supported Au particle with the same Au loading was prepared by an impregnation method. Bare and Au-loaded MCM-41s were also characterized by N_2 adsorption measurement and XRD (Fig. 4). There is no significant difference in N_2 adsorption-desorption isotherms (Fig. 4a); BET surface area and

NLDFT pore diameter of bare MCM-41 are 760 m^2 g^{-1} and 4.5 nm, and those of Au-loaded MCM-41 are 750 m^2 g^{-1} and 4.3 nm. In contrast, new sharp diffractions are clearly observed in high-angle region of the XRD pattern after gold metal formation (Fig. 4b). They are assigned to (111), (200), (220), (311), and (222) planes on the basis of the fcc structure of gold metal. The crystallite size was determined by the Debye-Scherrer's equation for the (111) diffraction to be ca. 38 nm. Aggregation of small AuNPs formed inside mesopores preferably occurred to form large-sized AuNPs on the outer surface of MCM-41 particles even though Au cations were homogeneously immobilized on the silica surface before thermal reduction. This phenomenon can be induced by weak interaction of AuNPs with silica surface. It should be noted that these large Au particles are not formed on BPy-PMO.

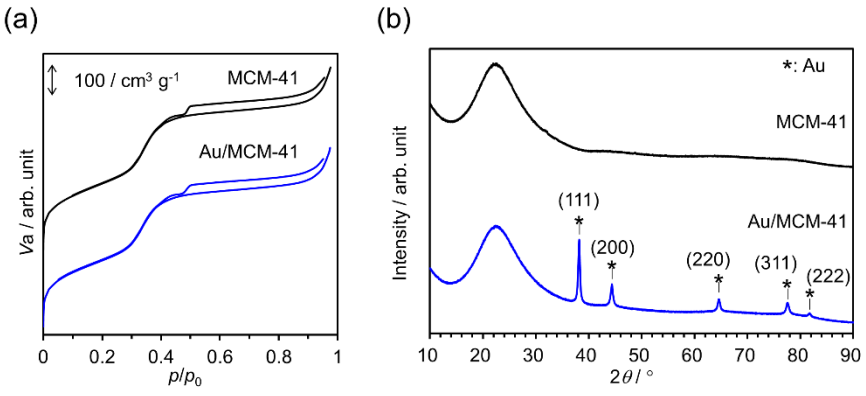

Fig. 4. (a) N_2 adsorption isotherms and (b) XRD patterns of bare (black line) and Au-loaded MCM-41 (blue line).

The formation of AuNPs on BPy-PMO was further evaluated in more details by UV/Vis DRS and TEM measurements (Fig. 5). A plasmon absorption peak derived from AuNPs appeared around 530 nm in AuNPs/BPy-PMO (Fig. 5a). TEM image of AuNPs/BPy-PMO gives direct information for AuNPs formation with an average size of 3.8 nm (Fig. 5b) and their homogeneous distribution inside and outside of mesopores whereas some large AuNPs in size of 6-8 nm are simultaneously observed on the external surface in Fig. 5b. AuNPs formed inside mesopores of BPy-PMO are highly stabilized with strong interaction between metallic Au and pore wall of BPy-PMO, which restricts formation of large-sized AuNPs typically observed for MCM-41 as shown above. In addition, mesopores effectively prevent growing the size of AuNPs below the poresize (4.4 nm). Thus, immobilization of AuNPs via the formation of gold complexes and subsequent H_2 reduction is definitely a simple and promising method to synthesize supported AuNPs on BPy-based PMO support in comparison with a conventional impregnation method.

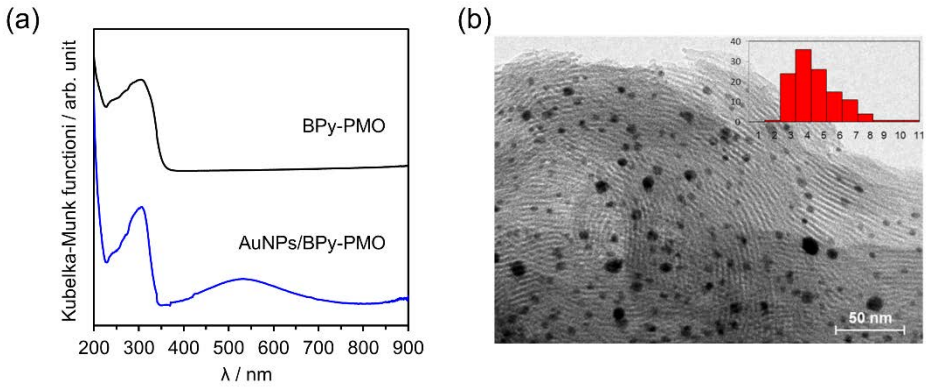

Fig. 5. (a) UV/Vis DRS spectra of bare and AuNPs/BPy-PMO and (b) TEM image of AuNPs/BPy-PMO.

Au L_3-edge XAFS measurement was conducted for the evaluation of Au species of AuNPs/BPy-PMO. Figs. 6a and 6b show XANES and Fourier transforms of EXAFS spectra of AuNPs/BPy-PMO and Au foil. These samples give similar edge energy (11919 eV), and EXAFS spectrum of AuNPs/BPy-PMO bears a great resemblance to that of Au foil, indicating complete reduction of Au complex on BPy-PMO and simultaneous formation of AuNPs. Weak and broad signals for metallic Au and the absence of small signals in range from 4-7 Å can be confirmed in the EXAFS spectrum of AuNPs/BPy-PMO. These features are characteristic of small AuNPs [29,30].

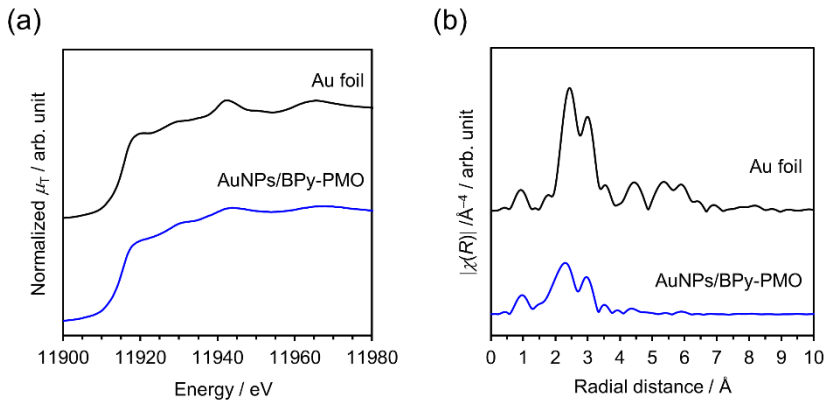

Fig. 6. (a) Au L_3-edge XANES and (b) Fourier transforms of EXAFS spectra for AuNPs/BPy-PMO (blue line) and Au foil (black line).

Finally, catalytic activity of the supported gold catalysts was examined using a test reaction, aerobic oxidation of benzaldehyde in water at 303 K (Fig. 7). Au/MCM-41 oxidized benzaldehyde to benzoic acid, giving 39% conversion and 22% yield toward benzoic acid. With the same Au loading, AuNPs/BPy-PMO afforded 91% conversion and 87% yield under the same conditions; yield of benzoic acid for AuNPs/BPy-PMO was approximately four times that for Au/MCM-41. Such a high activity can be ascribed to small Au nanoparticle on BPy-PMOs, which is frequently observed for catalytic reactions by supported Au nanoparticles [5,8]. The formation of small Au nanoparticles on BPy-PMO is potentially an effective strategy for the development of a highly active heterogeneous catalyst for various aerobic oxidation reactions.

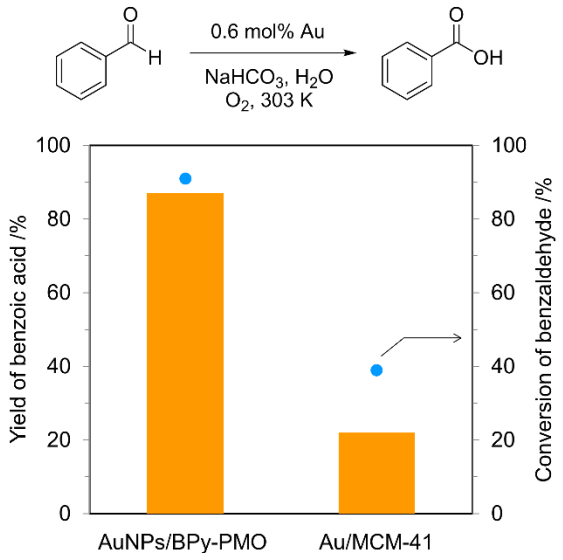

Fig 7. Aerobic oxidation of benzaldehyde in water with supported Au catalysts.

4. Conclusions

Complex formation and subsequent reduction is an effective method for the formation of small AuNPs with homogeneous distribution on 2,2'-bipyridine-based PMO material. Average diameter of AuNPs is estimated to be ca. 3.8 nm, which is much smaller than those formed on silica supports reported in the previous literatures. Mesoporous structure is one important factor controlling the size of AuNPs smaller than that of mesopores. AuNPs/BPy-PMO shows higher catalytic activity than Au/MCM-41 in oxidation of benzaldehyde. We believe that this methodology is useful to synthesize silica-supported AuNPs.

References

[1] M.-C. Daniel, D. Astruc, Chem. Rev. 104 (2004) 293-346.

[2] M. Turner, V. B. Golovko, O. P. H. Vaughan, P. Abdulkin, A. Berenguer-Murcia1, M. S. Tikhov, B. F. G. Johnson, R. M. Lambert, Nature (2008) 981-984.

[3] Y. Cheng, A. C. Samia, J. D. Meyers, I. Panagopoulos, B. Fei, C. Burda, J. Am. Chem. Soc. 130 (2008) 10643-10647.

[4] R. J. Tseng, J. Huang, J. Ouyang, R. B. Kaner, Y. Yang, Nano Lett. 5 (2005) 1077-1080.

[5] A. Corma, H. Garcia, Chem. Soc. Rev. 37 (2008) 2096-2126.

[6] M. Valden, X. Lai, D. W. Goodman, Science 281 (1998) 1647-1650.

[7] N. Ishito, K. Hara, K. Nakajima, A. Fukuoka, J. Energy Chem. 25 (2016) 306-310.

[8] M. Haruta, T. Kobayashi, H. Sano, N. Yamada, Chem. Lett. (1987) 405-406.

[9] S. Panigrahi, S. Basu, S. Praharaj, S. Pande, S. Jana, A. Pal, S. K. Ghosh, T. Pal, J. Phys. Chem. C 111 (2007) 4596-4605.

[10] H. Sakurai, A. Ueda, T. Kobayashi, M. Haruta, Chem. Commun. (1997) 271-272.

[11] M. Haruta, N. Yamada, T. Kobayahsi, S. Iijima, J. Catal. 115 (1989) 301-309.

[12] M. Y. Han, C. H. Quek, Langmuir 16 (2000) 362-367.

[13] M. Okumura, S. Tsubota, M. Haruta, J. Mol. Catal. A Chem. 199 (2003) 73-84.

[14] M. Brust, M. Walker, D. Bethell, D. J. Schiffrin, R. Whyman, J. Chem. Soc., Chem. Commun. (1994) 801-802.

[15] Y. Sunagawa, K. Yamamoto, H. Takahashi, A. Muramatsu, Catalysis Today 132 (2008) 81-87.

[16] P. D. Jadzinsky, G. Calero, C. J. Ackerson, D. A. Bushnell, R. D. Kornberg, Science 318 (2007) 430-433.

[17] W. W. Weare, S. M. Reed, M. G. Warner, J. E. Hutchison, J. Am. Chem. Soc. 122 (2000) 12890-12891.

[18] M. K. Corbierre, N. S. Cameron, M. Sutton, S. G. J. Mochrie, L. B. Lurio, A. Rühm, R. B. Lennox, J. Am. Chem. Soc. 123 (2001) 10411-10412.

[19] S. Inagaki, S. Guan, T. Ohsuna, O. Terasaki, Nature 416 (2002) 304-307.

[20] N. Mizoshita, T. Tani, S. Inagaki, Chem. Soc. Rev. 40 (2011) 789-800.

[21] S. Inagaki, O. Ohtani, Y. Goto, K. Okamoto, M. Ikai, K. Yamanaka, T. Tani, T. Okada, Angew. Chem. Int. Ed. 48 (2009) 4042-4046.

[22] M. Waki, N. Mizoshita, Y. Maegawa, T. Hasegawa, T. Tani, T. Shimada, S. Inagaki, Chem. Eur. J. 18 (2012) 1992-1998.

[23] M. Ohashi, M. Aoki, K. Yamanaka, K. Nakajima, T. Ohsuna, T. Tani, S. Inagaki, Chem. Eur. J. 15 (2009) 13041-13046.

[24] M. Waki, Y. Maegawa, K. Hara, Y. Goto, S. Shirai, Y. Yamada, N. Mizoshita, T. Tani, W. J. Chun, S. Muratsugu, M. Tada, A. Fukuoka, S. Inagaki, J. Am. Chem. Soc. 136 (2014) 4003-4011.

[25] Y. Maegawa, S. Inagaki, Dalton Trans. 44 (2015) 13007-13016.

[26] N. Ishito, H. Kobayashi, K. Nakajima, Y. Maegawa, S. Inagaki, K. Hara, A. Fukuoka, Chem. Eur. J. 21 (2015) 15564-15569.

[27] V. Amani, A. Abedi, S. Ghabeshi, H. R. Khavasi, S. M. Hosseini, N. Safari, Polyhedron 79 (2014) 104-115.

[28] M. Thommes, K. Kaneko, A.V. Neimark, J.P. Olivier, F. Rodríguez-Reinoso, J. Rouquerol, K.S.W. Sing, Pure Appl. Chem. 87 (2015) 1051-1069.

[29] H. Ikemoto, T. Miyanaga, Phys. Rev. Lett. 99 (2007) 165503.

[30] L. X. Chen, T. Rajh, Z. Wang, M. C. Thurnauer, J. Phys. Chem. B 101 (1997) 10688-10697.